

This work was written as part of one of the author's official duties as an Employee of the United States Government and is therefore a work of the United States Government. In accordance with 17 U.S.C. 105, no copyright protection is available for such works under U.S. Law.

Public Domain Mark 1.0

<https://creativecommons.org/publicdomain/mark/1.0/>

Access to this work was provided by the University of Maryland, Baltimore County (UMBC) ScholarWorks@UMBC digital repository on the Maryland Shared Open Access (MD-SOAR) platform.

Please provide feedback

Please support the ScholarWorks@UMBC repository by emailing scholarworks-group@umbc.edu and telling us what having access to this work means to you and why it's important to you. Thank you.

RELAXATION PROCESSES IN SOLAR WIND TURBULENCE

S. SERVIDIO¹, C. GURGIOLO², V. CARBONE¹, AND M. L. GOLDSTEIN³

¹ Dipartimento di Fisica, Università della Calabria, I-87030 Rende (CS), Italy; sergio.servidio@fis.unical.it

² Bitterroot Basic Research, Hamilton, MT 59840, USA

³ Heliospheric Physics Laboratory, Code 672, NASA Goddard Space Flight Center, Greenbelt, MD 20771, USA

Received 2014 May 6; accepted 2014 June 13; published 2014 June 27

ABSTRACT

Based on global conservation principles, magnetohydrodynamic (MHD) relaxation theory predicts the existence of several equilibria, such as the Taylor state or global dynamic alignment. These states are generally viewed as very long-time and large-scale equilibria, which emerge only after the termination of the turbulent cascade. As suggested by hydrodynamics and by recent MHD numerical simulations, relaxation processes can occur during the turbulent cascade that will manifest themselves as local patches of equilibrium-like configurations. Using multi-spacecraft analysis techniques in conjunction with *Cluster* data, we compute the current density and flow vorticity and for the first time demonstrate that these localized relaxation events are observed in the solar wind. Such events have important consequences for the statistics of plasma turbulence.

Key words: magnetohydrodynamics (MHD) – plasmas – solar wind – turbulence

Online-only material: color figures

1. INTRODUCTION

Intermittent turbulence and long-time relaxation processes represent two central features of magnetohydrodynamics (MHD). Turbulence, ubiquitous in fluids and in plasmas, cannot be fully described by simple models. In particular, a random-phase modeling of turbulence cannot capture the bursty and intermittent nature of the field gradients. Observations suggest that turbulent plasmas are characterized by high kurtosis of field fluctuations, multifractal behavior of the high-order structure functions, and other manifestations of intermittency that coexist with the cascade process (Sorriso-Valvo et al. 1999; Burlaga 2001; Bruno & Carbone 2013). Kurtosis and other higher-order moments were also studied in the context of compressible MHD with application to molecular clouds and to the diffuse interstellar medium (Burkhart et al. 2009, 2010). On a parallel path, the MHD theory of relaxation processes has been very successful in describing commonly observed features such as Taylor states (minimum energy states conserving magnetic helicity), selective decay, global dynamic alignment, and helical dynamo (Taylor 1974; Montgomery et al. 1978; Matthaeus & Goldstein 1982; Stribling & Matthaeus 1991; Carbone & Veltri 1992; Goldstein et al. 1995; Mininni et al. 2002, 2005). Relaxation is generally viewed as a slow consequence of multiple global ideal conservation principles leading as a final state to large-scale equilibria. Very little has been said about a possible link between intermittent turbulence, relaxation processes, and other critical features of MHD, such as the spectral anisotropy commonly observed in the presence of a mean magnetic field (Shebalin et al. 1983; Goldreich & Sridhar 1995; Cho & Vishniac 2000). The idea that local equilibrium patches are embedded in turbulence forms the basis of the present work.

It has been observed that in Navier–Stokes (NS) turbulence relaxation emerges quickly and locally, with important consequences for turbulence statistics (Pelz et al. 1985; Kraichnan & Panda 1988; Kerr 1987). In hydrodynamic experiments, in fact, it is commonly observed that the cascade produces states in which the velocity (\mathbf{v}) and vorticity ($\boldsymbol{\omega} = \nabla \times \mathbf{v}$) fields are strongly aligned (Tsinober et al. 1992). The latter is due to the

conservation of the global kinetic helicity $H_v = \langle \mathbf{v} \cdot \boldsymbol{\omega} \rangle$, where $\langle \dots \rangle$ denotes spatial averages. This alignment effect causes a suppression of the nonlinear interactions to levels much lower than in the case of Gaussian field modeling, suggesting that these local relaxation structures may be a crucial ingredient of the cascade (Moffatt 1984).

Here we establish multiple links between relaxation, turbulence, and intermittency in an astrophysical plasma. An observational precursor of the present work can be found in Osman et al. (2011), where, using data sets from the *Advanced Composition Explorer* spacecraft, it was shown that the solar wind velocity tends to align locally with the magnetic field. In a recent laboratory plasma experiment (Gray et al. 2013), it has also been observed that fluctuations in a plasma embedded in a magnetized cylinder exhibit a tendency to generate local force-free states. Using *Cluster* data and inspired by recent numerical experiments (Matthaeus et al. 2008; Servidio et al. 2008), we explore the possibility that several local and simultaneous relaxation processes occur in the turbulent solar wind. These consist of magnetic fields parallel to the current density (force-free), aligned velocity and magnetic fluctuations (Alfvénic), and correlated current and vorticity fields.

2. RELAXATION PROCESSES IN MHD

MHD is a leading model in the study of plasma turbulence at low frequencies and at spatial scales larger than the Larmor radius. The (incompressible) MHD equations are written as

$$\begin{aligned} \frac{\partial \mathbf{v}}{\partial t} &= \mathbf{v} \times \boldsymbol{\omega} + \mathbf{j} \times \mathbf{b} - \nabla P^* + \nu \nabla^2 \mathbf{v}, \\ \frac{\partial \mathbf{b}}{\partial t} &= \nabla \times (\mathbf{v} \times \mathbf{b}) + \eta \nabla^2 \mathbf{b}, \end{aligned} \quad (1)$$

where \mathbf{b} and $\mathbf{j} = \nabla \times \mathbf{b}$ are the magnetic and the current density field, respectively, $\nabla \cdot \mathbf{b} = 0$, ν and μ are viscous coefficients, and the pressure $P^* = p + (v^2/2)$ satisfies the incompressibility condition, namely $\nabla \cdot \mathbf{v} = 0$. (We confine our attention here to incompressible turbulence both to simplify

the discussion and because turbulence in the solar wind is in a nearly incompressible state, see, e.g., Marsch & Tu 1990.)

MHD relaxation involves both \mathbf{v} and \mathbf{b} fields and the family of equilibria known as Beltrami fields that can be obtained from variational principles (Montgomery et al. 1978). In particular, minimum energy states for MHD are obtained from the variational problem (Stribling & Matthaeus 1991)

$$\delta \int [(|\mathbf{v}|^2 + |\mathbf{b}|^2) - \alpha \mathbf{v} \cdot \mathbf{b} - \gamma \mathbf{a} \cdot \mathbf{b}] d^3x = 0, \quad (2)$$

where α and γ are constants, and \mathbf{a} is the potential vector such that $\mathbf{b} = \nabla \times \mathbf{a}$. Holding constant cross helicity $H_c = \langle \mathbf{v} \cdot \mathbf{b} \rangle$ and magnetic helicity $H_m = \langle \mathbf{a} \cdot \mathbf{b} \rangle$, Equation (2) minimizes the energy $E = \langle |\mathbf{v}|^2 + |\mathbf{b}|^2 \rangle$. The solutions of Equation (2) can be summarized as

$$\mathbf{v} = c_1 \mathbf{b} = c_2 \mathbf{j} = c_3 \boldsymbol{\omega}, \quad (3)$$

where c_j are combinations of α and γ . Note that the above Beltrami solutions include the Taylor force-free state, $\mathbf{j} \sim \mathbf{b}$ (Taylor 1974), and the Alfvén solutions, with $\mathbf{v} \sim \mathbf{b}$. Global Alfvénic states are sometimes observed in the solar wind (Belcher & Davis 1971; Dobrowolny et al. 1980; Osman et al. 2011). Steady, driven MHD also shows alignment at small scales (Mason et al. 2006; Matthaeus et al. 2008). It is crucial to note that solutions given by Equation (3) cancel the nonlinear terms in Equations (1), and are therefore equilibria.

Decaying simulations of MHD turbulence show that, after a long time, an asymptotic equilibrium is reached, characterized by long wavelength states that can be force-free and/or Alfvénic (Montgomery et al. 1978; Stribling & Matthaeus 1991; Mininni et al. 2005). Generally, global processes of relaxation require many characteristic times, after which energy is dissipated at small scales. Recently, Servidio et al. (2008) have shown through MHD simulations that alignment processes can also appear locally and very quickly during the cascade process. In particular, coherent structures, characterized by the force-free and the Alfvénic states, spontaneously emerge in turbulence. This may be due to the fact that the growing time of these inertial range patterns are comparable to the nonlinear times, which are much smaller than the global relaxation times. Although these phenomena have not been numerically investigated in a driven stationary case, there is supporting evidence that these patches, similar to the situation in NS turbulence, cause a suppression of the strength of the nonlinear interactions.

In analogy with previous theoretical studies (Kraichnan & Panda 1988; Servidio et al. 2008), we investigate the relaxation principle by computing the probability distribution functions (PDFs) of the cosine angle:

$$\cos \theta = \frac{\mathbf{f} \cdot \mathbf{g}}{|\mathbf{f}| |\mathbf{g}|}, \quad (4)$$

where $\{\mathbf{f}, \mathbf{g}\}$ represents one of $\{\mathbf{v}, \mathbf{b}\}$, $\{\mathbf{v}, \boldsymbol{\omega}\}$, $\{\mathbf{j}, \mathbf{b}\}$, and $\{\mathbf{j}, \boldsymbol{\omega}\}$. Note that the exact Beltrami correlations would be manifested as peaked distributions at $\cos \theta = \pm 1$. The presence of a finite cross and/or magnetic helicity will produce a skewness in the distribution in the cosines. On the other hand, Gaussian uncorrelated variables produce a flat distribution of $\text{PDF}(\cos \theta) = 0.5$. The latter value is simply related to the bounded nature of the cosine angle, $-1 \leq \cos \theta \leq 1$, and to the definition of PDF, $\int_{-1}^1 \text{PDF}(\cos \theta) d \cos \theta = 1$ (Matthaeus et al. 2008; Servidio et al. 2008). The appearance of Beltrami flows is implicitly associated with patterns where nonlinearity is

suppressed, and where the energy cascade is therefore inhibited (Kerr 1987). Alignment is strong in these regions due to a local conservation of magnetic and cross helicity. Note also that the presence of a very intense guide field, B_0 , may break the conservation of the magnetic helicity (Shebalin 2006; Stribling & Matthaeus 1991; Stribling et al. 1994), although in the case of a weak guide magnetic field (with respect to the level of fluctuations) the magnetic helicity may be considered weakly conserved (Servidio & Carbone 2005).

3. SOLAR WIND ANALYSES

To investigate MHD turbulent relaxation summarized by Equations (3) and (4), both the fields and their respective curls are needed. Direct observations of vorticity and current density require volumetric measurements that involve simultaneous measurements at a minimum of four non-coplanar positions (Dunlop et al. 2002). This was not possible until the launch of *Cluster*. With *Cluster* data, measurements of three-dimensional properties and symmetries of the magnetic fluctuations have been possible using data from the Flux Gate Magnetometer (FGM) and Spatio-Temporal Analysis of Field Fluctuations experiments (see, e.g., Narita et al. 2006; Sahraoui et al. 2010). The thermal electron experiment on *Cluster* (the Plasma Electron and Current Experiment (PEACE)) has been used to measure electron vorticity by using computed spatial derivatives of the electron moments (Gurgiolo et al. 2010, 2011). Note that at low frequencies (i.e., in the MHD limit) the latter represent a good measure of the proton vorticity as well $\omega_e \sim \omega_p \equiv \omega$. This correspondence has been confirmed from previous analysis that compared electron moments from PEACE with ion moments from the Cluster Ion Spectrometry (CIS) experiment (Gurgiolo et al. 2010). The current density has been computed using a similar multi-spacecraft technique. To summarize, the present work uses data from several *Cluster* experiments: electron data come from PEACE, while data from FGM, electric field and waves, CIS, and WHISPER are used to describe local conditions, to verify the electron data, and to support the conclusions. The data cadence has been synchronized to be 4 s and both field and velocity measurements have been interpolated to the geometric center of the tetrahedron.

Data have been carefully screened to meet multiple criteria. We have checked that the measurements are not in regions magnetically connected to the bow shock by making sure that there is no evidence of “return” electrons (i.e., electrons that have been reflected off or leaked through the bow shock, see, e.g., Wu 1984; Gosling et al. 1989; Larson et al. 1996). Within the analyzed intervals the *Cluster* spacecraft are in a good tetrahedral configuration. In addition, errors such as timing and position uncertainties, moment computation errors, inter-spacecraft calibration, and errors in the linear approximation (used for computing the derivatives) have been carefully checked and handled. A detailed discussion of many of the above error sources can be found in Chanteur (1998), Vogt & Paschmann (1998), and how they were approached in the context of the present analysis is discussed in Gurgiolo et al. (2010). The error estimated on the computations of plasma moments are of order of 6%, while for spatial derivatives the error is of the order of 15%.

We report on two time periods, 2003 March 2 16:10–18:30 UT and 2006 January 16 4:20–5:50 UT. These time intervals meet all of the requirements listed above. Figure 1 shows the power spectra of the magnetic field and the velocity for the 2003 time period. The higher frequencies in the plots extend to 0.125 Hz (the Nyquist frequency). The lower frequencies correspond

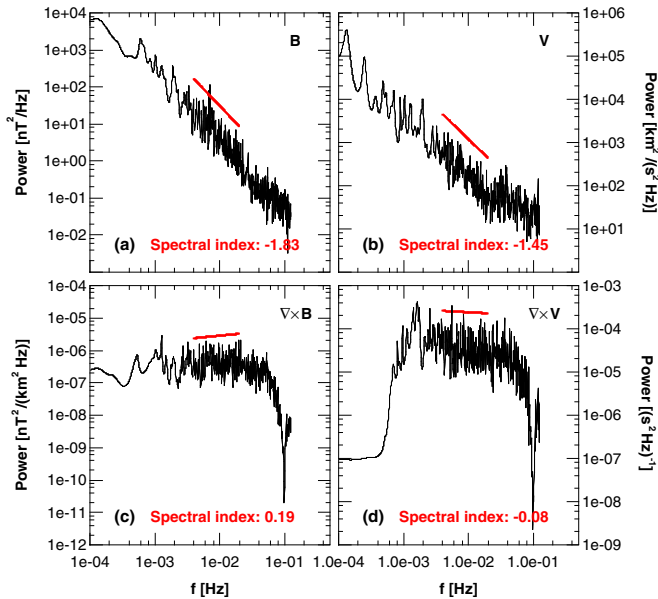


Figure 1. Power spectra of the magnetic field (a), velocity (b), current density (c), and vorticity (d) for the 2003 time period. The current density has been obtained with a low pass filter ($f < 0.05$ Hz), while the vorticity with a bandpass filter ($0.0005 < f < 0.05$ Hz). The straight (red) lines are least-squares fits (which have been offset), and the slopes are given at the bottom of the plots. (A color version of this figure is available in the online journal.)

to timescales on the order of the correlation time, which at this radial distance is approximately 1 hr. The magnetic field spectrum is slightly steeper than the velocity spectrum (see Bruno & Carbone 2013; Podesta et al. 2007).

Prior to computing the cosine angles in Equation (4), it is necessary to precondition the data. The very low-frequency components need to be filtered out of the mean solar wind speed before the computation of the vorticity. The presence of these low frequencies may swamp the velocity fluctuations, especially in the radial components. This is done by applying a high pass filter to the velocity data (a filter frequency 0.0005 Hz) to remove the mean flow. Also, the presence of high-frequency noise in both $\nabla \times \mathbf{v}$ and $\nabla \times \mathbf{b}$ may affect gradients and act to suppress the existence of alignment effects. The latter problem can be easily rectified by using a low pass filter to remove frequencies above 0.04 Hz. Figure 1 also shows the spectra of the current density (panel (c)) and the vorticity (panel (d)). Note that the power spectrum of the vortical fields has a flatter slope than do the original fields, consistent with the small-scale nature of the gradients. The velocity and magnetic spectra are generally consistent with the Kolmogorov expectation for isotropic fluid turbulence, showing a wide inertial range where the power $P(k) \sim k^{-5/3}$. Here k represents the wavenumber obtained using the Taylor frozen-in-flow hypothesis. From simple dimensional arguments, since the current density Fourier component $j_k \sim kb_k$, and analogously the vorticity $\omega_k \sim kv_k$, the power spectra of the vortical flows will scale as $k^2 P(k)$. In the inertial range, therefore, these gradient fields are consistent with an expectation of $\sim k^{-5/3+2} = k^{1/3}$.

To explore the possible presence of alignment patches in the turbulence, we computed the PDFs of the cosine angles defined by Equation (4), namely $\cos\theta_{vb}$, $\cos\theta_{jb}$, $\cos\theta_{v\omega}$, and $\cos\theta_{j\omega}$, for both solar wind periods. Note that the filtering procedure described before has been applied to all the fields prior to the computation of each cosine angle (Kerr 1987). As seen

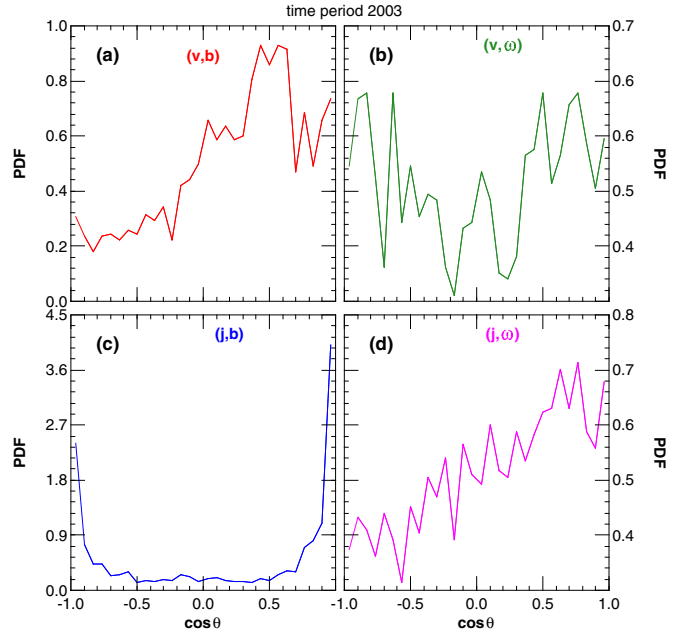


Figure 2. Probability distribution functions (PDFs) of the cosine angle defined in Equation (4) for the following alignments: (a) $\{\mathbf{v}, \mathbf{b}\}$, (b) $\{\mathbf{v}, \boldsymbol{\omega}\}$, (c) $\{\mathbf{j}, \mathbf{b}\}$, (d) $\{\mathbf{j}, \boldsymbol{\omega}\}$. The analysis has been performed for the 2003 data set. (A color version of this figure is available in the online journal.)

in Figure 2(a), the velocity and magnetic field in the 2003 time period exhibit a tendency to develop a highly aligned state, with a skewed probability toward $\cos\theta_{vb} = +1$. The skewness is due to the presence of a finite amount of cross helicity in the solar wind, while the more pronounced shape is related to the patchiness of the data. Fluctuations of the magnetic field and velocity alignment tend to have a pronounced probability at high correlations even if they have a lower global correlation (Matthaeus et al. 2008; Osman et al. 2011). These aligned states are not present in the correlation of the velocity with the vorticity, namely $\cos\theta_{v\omega}$. As seen in Figure 2(b), the distribution is very noisy and flat, with $\text{PDF}(\cos\theta_{v\omega}) \sim 0.5$, typical of random variables. The latter is due to the non-conservation of kinetic helicity in MHD turbulence, which is the main alignment in hydrodynamics (Kraichnan & Panda 1988).

The strongly peaked $\cos\theta_{jb}$ distribution at ± 1 in Figure 2(c) indicates the presence of local Taylor equilibria in the data that further confirms the prevalence of local relaxation processes. Note that most of the cosine angles are very weakly populated, and that this alignment, as in simulations, is the most common. As can be deduced from Equation (3), these Taylor states include the so-called local anisotropy (Cho & Vishniac 2000). It is well known in MHD theory that the presence of a mean field produces anisotropy, introducing a preferred direction along the guide field (Shebalin et al. 1983; Goldreich & Sridhar 1995; Cho et al. 2002; Cho & Lazarian 2003). In the latter case, the current density is parallel to the mean field. This phenomenon, even if it can be questioned in terms of the ergodic theorem (Matthaeus et al. 2012), can be viewed as a subclass of the Taylor states that can be manifest locally in solar wind turbulence.

Finally, in Figure 2(d), we plot the alignment between the current density and the vorticity. Viewed as a consequence of the Alfvénic relaxed states this suggests that current sheets and vortex filaments are correlated, which appears as a correlation between magnetic and velocity field intermittency. Obviously, this state is strongly related to the vb -correlation in

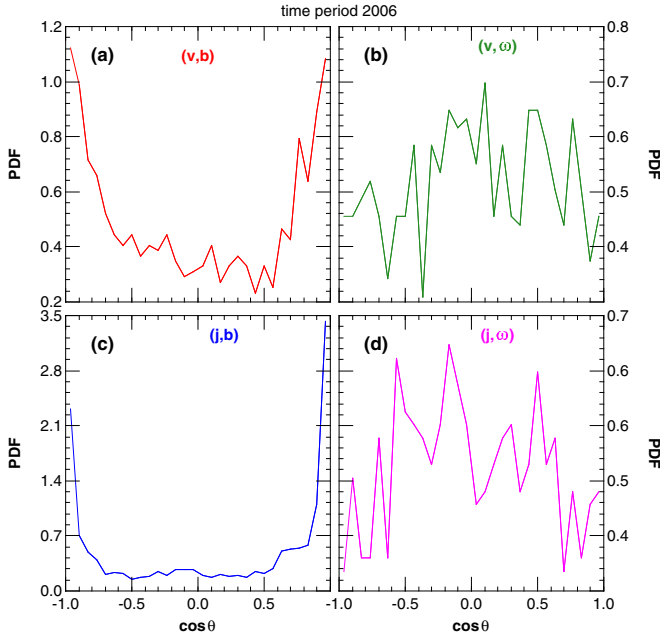


Figure 3. PDFs of the cosine angles for different alignments (see Figure 2) for the 2006 time interval.

(A color version of this figure is available in the online journal.)

Figure 2(a) except that it is much more sensitive to small-scale features.

In Figure 3, the same analysis has been performed for the 2006 sample. The typical double peaked shape of the alignment is now observed for both $\cos\theta_{vb}$ and $\cos\theta_{jb}$ as predicted in Servidio et al. (2008). The high probability of occurrence of Beltrami fields ($\cos\theta = \pm 1$) is associated with local equilibria that emerge from turbulence via rapid relaxation processes in which H_m and H_c are locally conserved. In contrast with hydrodynamics, in the MHD variational problem the kinetic helicity H_v is not conserved and therefore the $\{v, \omega\}$ alignment is lost in favor of the $\{v, b\}$ and the $\{j, b\}$ correlations. The main difference between the results in Figures 2 and 3 is in the distribution of $\cos\theta_{vb}$. As we will discuss below, with respect to 2006, the 2003 stream has a more pronounced and definite global cross-helicity value. Note also that the $\cos\theta_{j\omega}$ correlation is less visible in the 2006 time period, possibly due to both noise level and to a weaker statistical convergence.

To investigate whether the local Alfvénic states are correlated with the local Taylor equilibria, we produced a two-dimensional distribution of events in the plane given by $|\cos\theta_{jb}|$ and $|\cos\theta_{vb}|$, as shown in Figure 4, for both time periods. As it can be observed, especially in the 2006 case where the global cross helicity is lower, the primary v - b alignment correlates with the force-free states showing that equilibria in turbulence follow the complex relations summarized in Equation (3). This effect is related to the global relaxation processes where the final equilibrium solutions lie on an ellipse attractor (Ting et al. 1986; Stribling & Matthaeus 1991) as given by the following equation:

$$(1 - 2|\sigma_m|)^2 + (2\sigma_c)^2 = 1, \quad (5)$$

where $\sigma_c = H_c/E$ and $\sigma_m = H_m/E$. These normalized helicities indicate qualitatively the skewness of the cosine angles distributions. For example, for the 2003 time period, we obtained $\sigma_c \sim 0.7$, while, for Figure 3, $\sigma_c \sim -0.4$. On the contrary, we found negligible magnetic helicity, consistent with expectations of inertial range fluctuations (Matthaeus & Goldstein 1982).

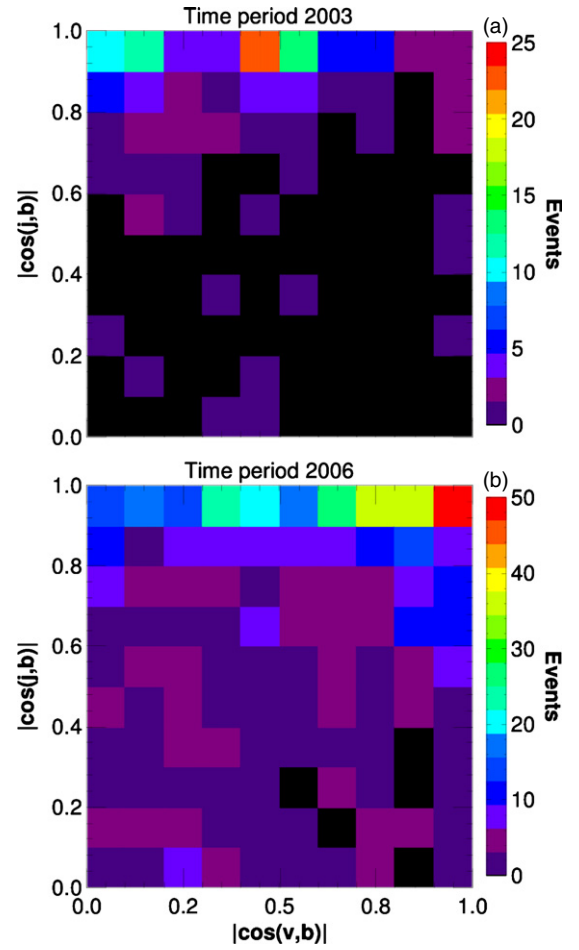


Figure 4. Joint distribution of events of $|\cos\theta_{jb}|$ vs. $|\cos\theta_{vb}|$, for the 2003 (a) and 2006 (b) time periods. As it can be seen, Alfvénic and Taylor alignment are correlated, revealing that Alfvénic patches are likely to be also force free.

(A color version of this figure is available in the online journal.)

4. DISCUSSION AND CONCLUSIONS

Using *Cluster* data to compute current density and flow vorticity we have shown that local alignments of several types are observed in the turbulent solar wind. Based on conservation of global energy, cross helicity, and magnetic helicity, MHD relaxation theory predicts the existence of several equilibrium states, such as the Taylor magnetic equilibrium and the global dynamic alignment. Previous theoretical work suggested that these states, which are generally viewed as very long-time and large-scale equilibria, appear only after the termination of the turbulent cascade. Here we have found that these patchy relaxation processes can coexist with the turbulent and intermittent cascade. Even in cases where the global correlation is null, $H_c \simeq H_m \simeq 0$, the cosine angles distribution may become concentrated near ± 1 . The presence of these equilibrium-like patterns requires that, statistically, the distributions of the fields, together with their gradients, become non-Gaussian. These results suggest that relaxation processes induce a suppression of nonlinearity in the solar wind. This “cellularization” of turbulence is not consistent with a superposition of random fields, and therefore involves phenomena such as intermittency and other non-Gaussian features, which necessarily involves high-order correlations that can be captured via multifractal analysis (She & Leveque 1994; Kowal et al. 2007; Bruno & Carbone 2013).

It is important to note, however, that some of these effects may be limited in the presence of very strong background magnetic fields since the conservation of H_m in this case is broken. However in the majority of the solar wind where the magnetic field is not that strong, the quasi-conservation of H_m may allow these force-free states as observed in Figures 2(c) and 3(c). Similar features, moreover, can manifest themselves in compressible turbulence. In certain regimes, indeed, the interstellar medium can be supersonic, and analogous phenomena can be investigated in the context of compressible relaxation theory (Ghosh & Matthaeus 1990).

Longer streams of solar wind data may help to better quantify the degree of local alignment, and to perform more direct comparison with simulations (Matthaeus et al. 2008). On the basis of the present results, however, nothing can be said about how (and where) these processes developed. They may in principle emerge during the solar wind expansion, or at the early stage of coronal dynamics and then slowly evolve as the wind flows outward. A deeper investigation of the role of the mean magnetic field and compressibility, as well as direct comparison with simulations, will be presented in future works.

This research was partially supported by the “Turboplasmas” project (Marie Curie FP7 PIRSES-2010- 269297), POR Calabria FSE 2007/2013, and the Cluster project at the Goddard Space Flight Center.

REFERENCES

- Belcher, J. W., & Davis, L. J. 1971, *JGR*, **76**, 3534
- Bruno, R., & Carbone, V. 2013, *LRSP*, **10**, 2
- Burkhart, B., Falceta-Gonçalves, D., Kowal, G., & Lazarian, A. 2009, *ApJ*, **693**, 250
- Burkhart, B., Stanimirović, S., Lazarian, A., & Kowal, G. 2010, *ApJ*, **708**, 1204
- Burlaga, L. F. 2001, *JGR*, **106**, 15917
- Carbone, V., & Veltri, P. 1992, *A&A*, **259**, 359
- Chanteur, G. 1998, in *Analysis Methods for Multi-spacecraft Data*, ed. G. Paschmann & P. W. Daly (Keplerlaan 1; Noordwijk, The Netherlands: ESA Publications Division), 349
- Cho, J., & Lazarian, A. 2003, *MNRAS*, **345**, 325
- Cho, J., Lazarian, A., & Vishniac, E. T. 2002, *ApJ*, **564**, 291
- Cho, J., & Vishniac, T. E. 2000, *ApJ*, **539**, 273
- Dobrowolny, M., Mangeney, A., & Veltri, P. 1980, *PhRvL*, **45**, 144
- Dunlop, M. W., Balogh, A., Glassmeier, K. H., & Robert, P. 2002, *JGR*, **107**, 1385
- Ghosh, S., & Matthaeus, W. H. 1990, *PhFIB*, **2**, 1520
- Goldreich, P., & Sridhar, S. 1995, *ApJ*, **438**, 763
- Goldstein, M. L., Roberts, D. A., & Matthaeus, W. H. 1995, *ARA&A*, **33**, 283
- Gosling, J. T., Thomsen, M. F., Bame, S. J., & Russell, C. T. 1989, *JGR*, **94**, 10011
- Gray, T., Brown, M. R., & Dandurand, D. 2013, *PhRvL*, **110**, 085002
- Gurgiolo, C., Goldstein, M. L., Viñas, A. F., & Fazakerley, A. N. 2010, *AnG*, **28**, 2187
- Gurgiolo, C., Goldstein, M. L., Viñas, A. F., Matthaeus, W. H., & Fazakerley, A. N. 2011, *AnG*, **29**, 1517
- Kerr, R. M. 1987, *PhRvL*, **59**, 783
- Kowal, G., Lazarian, A., & Beresnyak, A. 2007, *ApJ*, **658**, 423
- Kraichnan, R. H., & Panda, R. 1988, *PhFl*, **31**, 2395
- Larson, D. E., Lin, R. P., McFadden, J. P., et al. 1996, *GeoRL*, **23**, 2203
- Marsch, E., & Tu, C.-Y. 1990, *JGR*, **95**, 11945
- Mason, J., Cattaneo, F., & Boldyrev, S. 2006, *PhRvL*, **97**, 255002
- Matthaeus, W. H., & Goldstein, M. L. 1982, *JGR*, **87**, 6011
- Matthaeus, W. H., Pouquet, A., Mininni, P. D., Dmitruk, P., & Breech, B. 2008, *PhRvL*, **100**, 085003
- Matthaeus, W. H., Servidio, S., Dmitruk, P., et al. 2012, *ApJ*, **750**, 103
- Mininni, P. D., Gómez, D. O., & Mahajan, S. M. 2002, *ApJL*, **567**, L81
- Mininni, P. D., Montgomery, D. C., & Pouquet, A. G. 2005, *PhFl*, **17**, 035112
- Moffatt, H. K. 1984, in *Turbulence and Chaotic Phenomena in Fluids*, ed. T. Tatsumi (Amsterdam: North-Holland), 223
- Montgomery, D. C., Turner, L., & Vahala, G. 1978, *PhFl*, **21**, 757
- Narita, Y., Glassmeier, K. H., & Treumann, R. A. 2006, *PhRvL*, **97**, 191101
- Osman, K. T., Wan, M., Matthaeus, W. H., Breech, B., & Oughton, S. 2011, *ApJ*, **741**, 75
- Pelz, R. B., Yakhot, V., Orszag, S. A., Shtilman, L., & Levich, E. 1985, *PhRvL*, **54**, 2505
- Podesta, J. J., Roberts, D. A., & Goldstein, M. L. 2007, *ApJ*, **664**, 543
- Sahraoui, F., Goldstein, M. L., Belmont, G., Canu, P., & Rezeau, L. 2010, *PhRvL*, **105**, 131101
- Servidio, S., & Carbone, V. 2005, *PhRvL*, **95**, 045001
- Servidio, S., Matthaeus, W. H., & Dmitruk, P. 2008, *PhRvL*, **100**, 095005
- She, Z.-S., & Leveque, E. 1994, *PhRvL*, **72**, 336
- Shebalin, J. V. 2006, *JPIPh*, **72**, 507
- Shebalin, J. V., Matthaeus, W. H., & Montgomery, D. 1983, *JPIPh*, **29**, 525
- Sorriso-Valvo, L., Carbone, V., Veltri, P., Consolini, G., & Bruno, R. 1999, *GeoRL*, **26**, 1801
- Stribling, T., & Matthaeus, W. H. 1991, *PhFIB*, **3**, 1848
- Stribling, T., Matthaeus, W. H., & Ghosh, S. 1994, *JGR*, **99**, 2567
- Taylor, J. B. 1974, *PhRvL*, **33**, 1139
- Ting, A. C., Matthaeus, W. H., & Montgomery, D. 1986, *PhFl*, **29**, 3261
- Tsinober, A., Kit, E., & Dracos, T. 1992, *JFM*, **242**, 169
- Vogt, J., & Paschmann, G. 1998, in *Analysis Methods for Multi-spacecraft Data*, ed. G. Paschmann & P. W. Daly (Keplerlaan 1; Noordwijk, The Netherlands: ESA Publications Division), 419
- Wu, C. S. 1984, *JGR*, **89**, 8857